P H Y S I C A L   R E V I E W   L E T T E R S

Force Balance and Membrane Shedding at the Red-Blood-Cell Surface

Pierre Sens[1,*] and Nir Gov[2,†]

[1]*Physico-Chimie Théorique (CNRS UMR 7083), ESPCI, 10 rue Vauquelin, 75231 Paris Cedex 05-France*
[2]*Dept. of Chemical Physics The Weizmann Institute of Science, P.O.B. 26, Rehovot, Israel 76100*

During the aging of the red-blood cell, or under conditions of extreme echinocytosis, membrane is shed from the cell plasma membrane in the form of nanovesicles. We propose that this process is the result of the self-adaptation of the membrane surface area to the elastic stress imposed by the spectrin cytoskeleton, via the local buckling of membrane under increasing cytoskeleton stiffness. This model introduces the concept of force balance as a regulatory process at the cell membrane and quantitatively reproduces the rate of area loss in aging red-blood cells.

The membrane of red-blood cells (RBCs) is a fluid sheet of lipids and proteins, which is connected through node complexes to a two-dimensional cytoskeleton primarily composed of flexible spectrin protein filaments [1]. The shape and mechanical properties of the RBC result from a competition between the bending elasticity of the cell membrane and the shear and dilation elasticity of the cytoskeleton [2,3]. Because of the relative structural simplicity of the spectrin network, the RBC is a system of choice to study the co-organization of the lipid bilayer and the cytoskeleton cortex at the plasma membrane [2].

Over the natural lifespan of the RBC, the cell loses a large fraction of its membrane ($\sim 20\%$ over 120 days in humans and $\sim 10\%$ over 50 days in rabbits [4,5]) by the shedding of small vesicles containing hemoglobin but devoid of cytoskeleton [5–7]. The shed vesicles have a size (100–200 nm [1]) similar to the mesh-size of the underlying spectrin network [5,6,8], and may take the form of elongated cylinders [9]. The shedding of vesicles is also observed under conditions that trigger the transition into echinocyte shape, such as Adenosine triphosphate (ATP) depletion and Ca^{2+} loading [10]. In this case, the shedding of cytoskeleton-free vesicles often occurs at the tip of membrane spicules containing cytoskeleton [9,11,12]. The shedding of membrane area which we model here is crucial to the fate of the cell, as a decreasing surface-to-volume ratio is thought to be connected to the phagocytosis of old RBCs.

When the entire membrane of the RBC is removed under physiological conditions, the cytoskeleton shrinks to a 3- to 5-fold smaller area [13]. This indicates that the cytoskeleton is stretched by its attachment to the cell membrane [3,14], and therefore exerts a compression force on the membrane. As the cell ages, its observed stiffness increases by $\sim 20\%$ [15,16], as does the density of its cytoskeleton network by about ~ 30–40% [17]. A recent model [18] proposes that these changes may be related to the diminishing levels of ATP as the cell ages [19]. This model relates the ATP level to the degree of dissociations in the cytoskeleton network; lower ATP levels correspond to a

stronger cytoskeleton network, and results in larger compressive forces on the cell membrane. These forces are balanced by the membrane bending stress [3], which may either be of entropic origin (from constraints on the membrane thermal fluctuations), or resulting from an overall membrane curvature (blebbing). We show below that beyond a compression threshold, the membrane undergoes a buckling transition at the scale of the spectrin mesh-size, and one or a few membrane blebs grow in size in order to release the overall stress. We first analyze the buckling transition of a single membrane-cytoskeleton unit. The thermally fluctuating membrane is assumed flat at large length scales (we do not account for the global shape of the RBC), while the spectrin filaments are treated as phantom Hookean springs [20], attached at their ends to the mem-
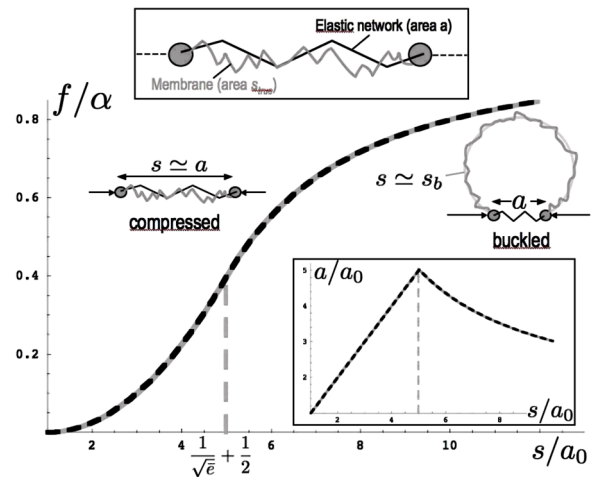

FIG. 1 (color online). Energy of a patch of fluctuating membrane of apparent area s fit to an elastic frame of rest area a_0. The energy shows an inflexion point when the membrane buckles. The gray line is the numerical optimization of Eq. (3) with Eq. (2) and the dashed line is the asymptotes Eq. (4), for $\alpha = 500$ ($\kappa = 20 k_B T$) and $\bar{e} = 5 10^{-2}$ ($e = 10^{-5}$ J/m^2 and $a_0 = (100$ nm$)^2$). Inset: The deformation of the cytoskeleton (area a) is maximal at the transition.

brane (Fig. 1). We then consider a large elastic network attached to a membrane and show that the lowest energy state beyond a critical compression strain consists of an essentially stress-free membrane connected to a large bleb which incorporates all the excess membrane area. We argue that such a state is never reached because the bleb pinches off the membrane to form a free vesicle before reaching large sizes. Finally, we relate our results to the observed shedding of vesicles during RBC aging.

Let us assume that one cytoskeleton unit, of area a, is connected to a patch of membrane of area s_{true} (Fig. 1), and constrains its fluctuations [21]. There exists an optimal unit area that leaves the fluctuations unconstrained. This area, which we call s, is the apparent area of a freely fluctuating membrane and is slightly smaller than the true area by a factor $s/s_{\text{true}} = [1 - (1/\alpha) \log s_{\text{true}}/l^2]$ [22]. Here, $\alpha \equiv 8\pi\kappa/k_BT$ is the bending energy of a closed sphere (compared to the thermal energy), and l a small size of order of the membrane thickness. If the membrane is stretched ($a > s$), or mildly compressed, it remains flat on average, and its free energy is [22,23]

$$f_{\text{fl}}[s, a] = \frac{\pi}{2} k_BT [e^{\alpha(a/s-1)} - 1 - \alpha(a/s - 1)]. \quad (1)$$

This energy is quadratic $[\sim \pi/2\alpha^2(a/s - 1)^2]$ for small compression $[\alpha(s/a - 1) < 1]$, and becomes linear $[\simeq \pi/2\alpha(1 - a/s)]$ for large compression. The energy of the flat compressed patch eventually becomes larger than the bending energy of a spherical cap, leading to the breaking of the up/down symmetry and the formation of a curved bleb. We investigate the buckling transition by assuming that a buckled membrane fluctuates around a mean shape defined by a spherical cap of area $s_b \geq a$, to be optimized (Fig. 1). The energy of a buckled patch reads

$$f_m[s, a] = 8\pi\kappa\left(1 - \frac{a}{s_b}\right) + f_{\text{fl}}[s, s_b]. \quad (2)$$

The first term is the bending energy of a spherical cap of area s_b on a frame of area a, and the second the energy of the thermal fluctuations [Eq. (1)], assumed unaffected by the curvature of the bleb. The membrane is flat on average if $s_b = a$ and is buckled if $s_b > a$. Comparing Eq. (1) and (2) shows that in the relevant limit ($\alpha \gg 1$), the optimal buckled area is $s_b \simeq s - 2a/\pi\alpha$, and buckling is to be expected for $s/a > 1 + 2/\pi\alpha$.

In addition to the membrane entropic elasticity f_m, the total energy of a membrane unit has a contribution from the cytoskeleton elasticity, treated here as a simple springlike quadratic energy:

$$f = \frac{1}{2} e a_0\left(\frac{a}{a_0} - 1\right)^2 + f_m[s, a]. \quad (3)$$

Here, e and a_0 are the stretching modulus and rest area of the cytoskeleton unit mesh. The full free energy for one patch [Eq. (3), with Eq. (2)] is to be optimized with respect to two areas: the buckled membrane area $s_b(<s)$ and the

area of the stretched cytoskeleton mesh $a(\geq a_0)$. The buckling transition is controlled by the area mismatch s/a_0 and the ratio of the typical cytoskeleton to membrane elasticity $\bar{e} \equiv ea_0/\alpha k_BT$. In the case of the RBC, we expect $\bar{e} \ll 1$ and the buckling transition is second order (the cytoskeleton area is continuous through the transition, Fig. 1-inset). The numerical minimization of the full energy is shown in Fig. 1. The buckling transition occurs for a critical mismatch $s/a_0 \simeq 1/\sqrt{\bar{e}}$ (for $\alpha \gg 1$ and $\bar{e} \ll 1$), and the optimal mesh-size and energy below and above the transition (subscripts "f" and "b," respectively) are

$$a_f = s; \qquad \frac{f_f}{\alpha} = \frac{1}{2}\bar{e}\left(\frac{s}{a_0} - 1\right)^2$$

$$a_b = a_0\left(1 + \frac{a_0}{\bar{e}s}\right); \qquad \frac{f_b}{\alpha} = 1 - \frac{a_0}{s} - \frac{a_0^2}{2\bar{e}s^2} \quad (4)$$

The area of the stretched cytoskeleton mesh, respectively, increases and decreases with increasing membrane area s below and above the buckling transition (Inset of Fig. 1).

We now proceed to describe the buckling instability of many connected patches. Under low compression, the membrane of the cell is equally shared by all cytoskeleton units, and if the membrane were not fluid, an increase of the cytoskeleton compressive stress would eventually lead to the buckling of every single membrane patch. Biological membranes are fluid, so once a unit buckles, it may grow into a large bleb by feeding from the excess area of the surrounding units. This reduces their energy without much increase of the energy of the bud, which saturates to the energy of a full sphere α for large area [Eq. (4)]. Mathematically, coexistence between flat and buckled units is allowed by the existence of an inflexion point in the energy of one isolated membrane patch [Fig. 1)].

Let us consider N membrane-cytoskeleton units similar to the one shown in Fig. 1, with total membrane area S. We investigate a membrane composed of $(N - 1)$ units of area s that are in the flat (unbuckled) state, plus one unit of area $S - (N - 1)s$, that may be buckled if such shape lowers the total energy:

$$F_{f,b}^{\text{tot}} = (N - 1)f_f(s) + f_{f,b}[S - (N - 1)s] \quad (5)$$

where the energies in the flat and buckled state (f_f and f_b, respectively) are given in Eq. (4). The parameter that controls the state of the membrane is the dimensionless average area per unit (area mismatch) S/Na_0, and the state of the membrane is unambiguously characterized by the area of the flat units s. For small area mismatch, the only equilibrium state corresponds to a uniform flat membrane with $s = S/N$. Upon increase of the mismatch, a local minimum of the total energy F_{tot} eventually appears for $s < S/N$, corresponding to an inhomogeneous membrane state with one buckled unit (Fig. 2). For large area mismatch, the uniform membrane becomes metastable and the optimal conformation is such that all the flat units are near their optimal area ($s \gtrsim a_0$), with all the excess area
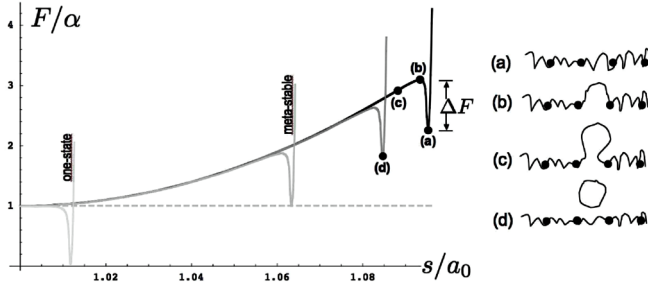
FIG. 2 (color online).   Energy of a collection of N membrane + cytoskeleton units as a function of the membrane area per unit s [from Eq. (5)]. Darker shades of gray corresponds to larger total membrane area S. The energy shows a narrow local minimum for an homogeneous flat membrane at $s = S/N$. A local minimum at $s \simeq a_0$ appears beyond the "one-state" point. It corresponds to stress-free units coexisting with a large membrane bleb. The homogeneous membrane (a) is globally unstable beyond the metastable point. After a waiting time depending on the nearness to the unstable line [Eq. (6)], a small bleb forms (b), grows (c), and stochastically pinches off the cell (d) reducing the total membrane area and leaving the system in a deeper local minimum until the next blebbing event. $N = 10^4$, $\bar{e} = 5 \times 10^{-2}$ and $S/Na_0 = 1.01$ (one-state), 1.063 (metastable), 1.085, and 1.095. The unstable point ($S/Na_0 = 4.98$) is not shown.

concentrated in the one nearly spherical bleb of energy $F_b^{\text{tot}} \simeq \alpha$.

The coexistence between flat and buckled states requires the equality of tensions: $\partial_s f_f(s) = \partial_s f_b[S - (N-1)s]$ ($\rightarrow \partial_s F_b^{\text{tot}} = 0$). The buckled state is the equilibrium state beyond a total area S_m (metastable point, Fig. 2) for which buckled and flat states have the same energy $F_b^{\text{tot}} = F_f^{\text{tot}} = N\alpha\bar{e}/2[S_m/(Na_0) - 1]^2$. Although it is thermodynamically favorable to form a large bleb devoid of cytoskeleton for $S > S_m$, this process requires an activation energy ΔF (see Fig. 2). The energy barrier is very large (of order $\alpha \simeq 500k_BT$ close to $S = S_m$, decreases with increasing area mismatch, and vanishes at the "unstable" point $S = S_u$ for which every single unit is unstable with respect to buckling. Depending on kinetics, buckling will thus occur somewhere between the metastable and unstable mismatches S_m and S_u which, in the relevant limit ($\bar{e} \ll 1$ and $N\bar{e} \gg 1$), are given by

$$\frac{S_m}{Na_0} \simeq 1 + \sqrt{\frac{2}{\bar{e}N}}; \qquad \frac{S_u}{Na_0} \simeq \frac{1}{\sqrt{\bar{e}}}. \qquad (6)$$

After the buckling of one membrane unit [Fig. 2(b)], the system then evolves downhill [Fig. 2(c)] toward its global equilibrium state, which corresponds to a large bleb in coexistence with stress-free units ($s \simeq a_0$). The "equilibrium bleb" takes all the excess area, and should thus be very large (area of order $a_0\sqrt{N/\bar{e}}$ if buckling occurs at the metastable point and $a_0N/\sqrt{\bar{e}}$ near the unstable point).

Although such large blebs are observed in blebbing cells, they generally involve the unbinding of large patches ($\sim \mu m^2$) of membrane from the cytoskeleton [24] and do not bud off the cell. In aging RBC, small spherical or cylindrical vesicles of size comparable to the cytoskeleton mesh-size [$\sim (100 \text{ nm})^2$] are being shed. This phenomenon could have a kinetic origin and be explained by the following simple argument. Once a unit membrane has buckled, it initially grows to form a hemispherical cap (of bending energy $\alpha/2$), from which it may grow further into a shape approaching either a fully formed sphere or a cylinder. The bending energy of the cylinder [$\sim \alpha(s_b/(16a) + 3/8$] is smaller than the energy of the sphere [$\sim \alpha(1 - a/s_b)$], as long as $s_b < 8a$, so we argue that the buckled unit should initially grow as a cylinder.

The growing bleb should undergo large fluctuations, owing to the fact that the membrane is under small (or even negative) surface tension. One may thus expect the high curvature neck connecting the bleb to the cell membrane [Fig. 2(c)] to eventually close and the bleb to pinch off before reaching a large size, in agreement with the experimental observations. Vesicle scission is expected to be much faster than the RBC aging process and could be promoted by phase separation of lipids and proteins within the membrane of the bleb [25]. Once shedding has occurred, the system finds itself in a new (deeper) local energy minimum [Fig. 2(d)], corresponding to the reduced total membrane area S.

In the context of the RBC, the cytoskeleton stiffness e continuously increases with time [15,16]. Correspondingly, the energy barrier that keeps the cell in the stressed state decreases and the probability of a stochastic buckling event, followed by vesicle shedding, increases. The evolution of the membrane area with time can be written as a Kramer process of passage over a potential barrier [26]:

$$\frac{\partial S}{\partial t} = \frac{s_v}{\tau_0} e^{-\Delta F[S, e(t)]/k_BT} \qquad (7)$$

where $s_v \simeq 5a_0$ is the size of the shed vesicle, $\tau_0 \sim 0.1$ ms is the typical time scale for membrane fluctuations of wavelength of the cytoskeleton mesh-size [18], and ΔF is the area-dependent energy barrier (Fig. 2). Note that nonthermal perturbations to the RBC, e.g., due to mechanical shear and metabolic processes [18], may also contribute to excite the system over the energy barrier in Eq. (7). Figure 3 shows the evolution of the cell membrane area for various rates of cytoskeleton stiffening. After a short transient regime, the buckling rate adjusts to the rate of cytoskeleton stiffening, as the pinching off of the buckled membrane reduces the RBC area and stabilizes the flat state until further stiffening.

Buckling occurs close to the unstable point ($S \simeq S_u$) in the limit of a very fast ATP depletion rate, and at the metastable point ($S = S_m$) for unrealistically slow rate
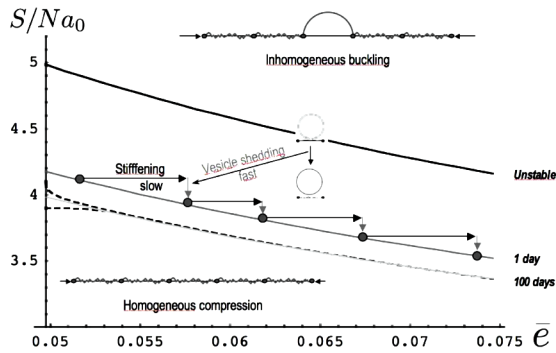
FIG. 3 (color online). "Nonequilibrium Phase diagram" for RBC buckling. Cells with large membrane area (*y*-axis) are unstable to buckling. The critical area for buckling depends upon the cytoskeleton stiffness (*x*-axis), and the stiffening rate. Aging RBCs follow trajectories (dashed lines, for two initial conditions) that are solutions of Eq. (7), showing cytoskeleton stiffening and the loss of membrane area (through vesiculation, vertical arrows). After a short transient regime, the trajectories are such that the rate of vesicle shedding matches the rate of cytoskeleton stiffening (gray lines, see text). Three rates are represented (10% increase of cytoskeleton stifness in: 100 days, 1 d, and the unstable line, Eq. (6), corresponding to infinitely fast stiffening). Parameters are the same as Figs. 1 and 2.

(not shown). For intermediary rates, the membrane area is solution of $\Delta F[S, e(t)] = k_B T \log \frac{s_v}{Na} \frac{e/\tau_0}{\partial_t e}$. Near the unstable line, an increase δe of the cytoskeleton stiffness leads to a decrease $\delta S = -S \delta e/(2e)$ of membrane area [Eq. (6)]. The observed rate of membrane shedding from aging RBCs is 20% in 100 days, which translates to about one 100 nm-sized vesicle an hour, consistent with an energy barrier at the transition $\Delta F \simeq 15 k_B T$. We predict this loss of area to correlate with a 40% stiffening of the spectrin cytoskeleton (Fig. 3), in agreement with mechanical and structural measurements [15–17]. The calculated metastable excess membrane area $S/Na_0 \simeq 4$ (Fig. 3) also agrees well with experimental observation [13].

We conclude that the compression forces produced by an elastic network on an attached fluid membrane may lead to buckling and eventual vesiculation of the membrane. These conditions occur under slow RBC aging, during ATP depletion or Ca^{2+} loading, all of which result in cytoskeleton stiffening [18]. Note that Ca^{2+} loading occurs regularly at the neural synapse, where internal vesicles respond by fusing and releasing their content [27]. Our work shows that a cortical network may act to mechanically produces small vesicles, in a process entirely distinct from the classical Clathrin-based budding mechanism. It may therefore be relevant to some of the many biological systems containing fluid membranes with an attached elastic network.

*Electronic mail: pierre.sens@espci.fr
†Electronic mail: nirgov@wisemail.weizmann.ac.il

[1] V. Bennett, Biochim. Biophys. Acta **988**, 107 (1989).
[2] N. Mohandas and E. Evans, Annu. Rev. Biophys. Biomol. Struct. **23**, 787 (1994).
[3] N. G. Lim, M. Wortis, and R. Mukhopadhyay, Proc. Natl. Acad. Sci. U.S.A. **99**, 16 766 (2002).
[4] R. E. Waugh, M. Narla, C. W. Jackson, T. J. Mueller, T. Suzuki, and G. L. Dale, Blood **79**, 1351 (1992).
[5] J. M. Werre, F. L. Willekens, F. H. Bosch, L. D. de Haans, S. G. van der Vegt, A. G. van den Bos, and G. J. Bosman, Cell. Mol. Biol. (Noisy-le-grand) **50**, 139 (2004).
[6] H. U. Lutz, S.-C. Liu, and J. Palek, J. Cell Biol. **73**, 548 (1977).
[7] L. Backman, J. B. Jonasson, and P. Hörstedt, Mol. Membr. Biol. **15**, 27 (1998).
[8] U. Salzer, P. Hinterdorfer, U. Hunger, C. Borken, and R. Prohaska, Blood **99**, 2569 (2002).
[9] A. Iglič, P. Veranič, K. Jezernikb, M. Fošnarič, B. Kamina, H. Hägerstrandc, and V. Kralj-Iglič, Bioelectrochem. Bioenerg. **62**, 159 (2004).
[10] R. Bucki, C. Bachelot-Loza, A. Zachowski, F. Giraud, and J.-C. Sulpice, Biochemistry **37**, 15 383 (1998).
[11] S.-C. Liu, L. H. Derick, M. A. Duquette, and J. Palek, Eur. J. Cell Biol. **49**, 358 (1989).
[12] W. H. Reinhart and S. Chien, Am. J. Hematol. **24**, 1 (1987).
[13] S. Tuvia, S. Levin, A. Bitler, and R. Korenstein, J. Cell Biol. **141**, 1551 (1998); S. Levin and R. Korenstein, Biophys. J. **60**, 733 (1991).
[14] D. E. Discher, D. H. Boal, and S. K. Boey, Biophys. J. **75**, 1584 (1998).
[15] K. Fricke and E. Sackmann, Biochim. Biophys. Acta. **803**, 145 (1984).
[16] S. P. Sutera *et al.*, Blood **65**, 275 (1985).
[17] F. Liu, H. Mizukami, S. Sarnaik, and A. Ostafin, J. Struct. Biol. **150**, 200 (2005).
[18] N. Gov and S. Safran, Biophys. J. **88**, 1859 (2005).
[19] Z. Tochner, J. Benbassat, and C. Hershko, Scand. J. Haematol. **14**, 377 (1975).
[20] C. Dubus and J.-B. Fournier, Europhys. Lett. **75**, 181 (2006).
[21] J. B. Fournier, D. Lacoste, and E. Raphaël, Phys. Rev. Lett. **92**, 018102 (2004).
[22] W. Helfrich and R. Servus, Nuovo Cimento Soc. Ital. Fis. **3D**, 137 (1984).
[23] P. Sens and S. A. Safran, Europhys. Lett. **43**, 95 (1998).
[24] M. P. Sheetz, J. E. Sable, and H.-G. Döbereiner, Annu. Rev. Biophys. Biomol. Struct. **35**, 417 (2006).
[25] A. Roux, D. Cuvelier, P. Nassoy, J. Prost, P. Bassereau, and B. Goud, EMBO J. **24**, 1537 (2005).
[26] N. G. Van Kampen, *Stochastic Processes in Physics and Chemistry* (North-Holland, Amsterdam, 2004).
[27] See for example: J. E. Richmond and K. S. Broadie, Curr. Opin. Neurobiol. **12**, 499 (2002).